Final Technical Report
University Of Wisconsin-Madison

(To be completed by RSP or the Department)

Project Title:	**Clouds of Uranus and Neptune**
Award Number:	**NNX09AB67G**
UW Account Number:	**PRJ23WQ**
For the Period of:	**1/1/2009-12/31/2011**
Principal Investigator:	**Lawrence Sromovsky**
Date Submitted:	**19 April 2012**
Location:	**University of Wisconsin Madison** **Space Science and Engineering Center** **1225 West Dayton Street** **Madison, WI 53706**
Reports will be sent to:	**Philippe Crane** **philippe.crane@nasa.gov** **NSSC-Grant-Report@mail.nasa.gov**
SSEC Number (Internal)	***6457*** **I:/jennyh/Reports/6457Yr2.doc**

(To be completed by the Principal Investigator)

Inventions Report:

☒ No Inventions resulted from this award
☐ Yes

Inventory Report:

☒ No federally owned equipment is in the custody of the PI
☐ Yes

Publications: (Please list)

Peer-reviewed Publications:

Sromovsky, L. A., P. M. Fry, and J. H. Kim. 2011. Methane on Uranus: The case for a compact CH_4 cloud layer at low latitudes and a severe CH_4 depletion at high latitudes based on re-analysis of Voyager occultation analysis and STIS spectroscopy. *Icarus* **215**, 292-312. (Partly supported by NASA Outer Planets Research Grant NNG05GG93G.)

Sromovsky, L. A., P. M. Fry, V. Boudon, A. Campargue, and A. Nikitin, 2012. Comparison of line-by-line and band models of near-IR methane absorption applied to outer planet atmospheres, *Icarus* **218**, 1-23. (Partly supported by Planetary Astronomy grant NNX08A051G.)

Sromovsky, L. A., P. M. Fry, H. B. Hammel, I. de Pater, K. A. Rages, M. R. Showalter, W. J. Merline, P. Tamblyn, C. Neyman, J.-L. Margot, J. Fang, F. Colas, J.-L. Dauvergne, J. M. Gomez-Forrellad, R. Hueso, A. Sanchez-Lavega, and T. Stallard. 2012. Episodic bright and dark spots on Uranus. *Icarus* **in press**. (Partly supported by Planetary Astronomy grant NNX08A051G and a small grant from the Space Telescope Science Institute to support TOO observations.)

Kim, J. H., L. A. Sromovsky, and P. M. Fry. 2012. The vertical structure of deep discrete cloud features on Uranus. In preparation for submission to Icarus. (This grant provided only partial support.)

Conference Papers:

Fry, P.M. and L. A. Sromovsky, Implications of New Methane Absorption Coefficients on Uranus Vertical Structure Derived from Near-IR Spectra 2009. Bull. Am. Astron. Soc. 41, p 1010.

Kim, J. H., L. A. Sromovsky, and P. M. Fry, Radiative Transfer Modeling on the Atmosphere of Uranus. 2010. Bull. Am. Astron. Soc. 41, p 1022. (Supported mainly by a grant from the Space Telescope Science Institute.)

Kim, J. H., Sromovsky, L. A., Fry, P.M. 2011. The vertical structure of deep cloud features on Uranus. EPSC-DPS Joint Meeting 2011, 1392. (Supported mainly by a grant from the Space Telescope Science Institute.)

Sromovsky, L. A., Fry, P. M., Kim, J. H. 2011. High-latitude depletion of methane on Uranus. EPSC-DPS Joint Meeting 2011, 1461. (Partly supported by NASA Outer Planets Research Grant NNG05GG93G.)

Sromovsky, L. A., Fry, P. M., Kim, J. H. 2011. The case for a compact methane cloud on Uranus based on a reanalysis of the Voyager 2 radio occultation and STIS Spectra. EPSC-DPS Joint Meeting 2011, 1422. (Partly supported by NASA Outer Planets Research Grant NNG05GG93G.)

Sromovsky, L. A., Fry, P. M. 2011. Comparison of line-by-line and band-model calculations of methane absorption in outer planet atmospheres. EPSC-DPS Joint Meeting 2011, 1384. (Partly supported by Planetary Astronomy grant NNX08A051G.)

Summary of Technical Effort: (Usually several paragraphs. Please feel free to attach additional pages if you wish.)

OBJECTIVES: Our main objectives are to determine what the clouds of Uranus and Neptune are composed of, what their parent gases are, how they respond to seasonal forcing, how cloud bands differ from discrete features, and what their short-term and long-term variations are. The high-quality observations to be used to further these aims are Hubble Space Telescope observations at visible and near-IR wavelengths and intensive ground-based observations of Uranus at near-IR wavelengths. More recent observations include NICMOS observations made in 1997, as well as Cycle 17 observations both General Observer (Sromovsky PI) and Snap (Rages PI) programs, although the initial analysis of Cycle 17 observations will be funded by STScI grants.

RESULTS:

The main results of this effort were (1) analysis of STIS spectra in combination with Voyager radio occultation results to develop new constraints on Uranus cloud structure, (2) improvements of line-by-line near-IR models of methane absorption, and comparison of line-by-line and near-IR band models as applied to outer planet atmospheres, and (3) application of new absorption coefficients to derive altitudes of discrete cloud features on Uranus and constraints on their composition.

Motivation for modeling STIS spectra. We began with modeling of STIS observations, which provides spatially resolved spectra over half of the Uranus disk during 2002. These observations were well fit by Karkoschka and Tomasko (Icarus 202, 287-309, 2009), henceforth referred to as **KT09**, but are worth reanalysis for several reasons: (1) we can include accurate Raman scattering, which was only roughly approximated in the prior analysis, (2) the degree to which parameters of the model are constrained by the observations is not well defined and thus uniqueness is a serious issue and other models are likely possible, (3) the assumed wavelength dependence of the phase function is non-physical in the sense that most particles produce increased backscatter with increasing wavelength rather than the opposite, which is the characteristic of the KT09 model, making it worthwhile to test

other solution with more plausible physical characteristics, (3) recent analysis of IR spectral observations by Irwin et al. (2010, Icarus 208, 913-926) suggest a compact cloud layer with pressure increasing towards the equator instead of the vertically diffuse layers and latitude-independent vertical boundaries of the KT09 model, (4) the vertical scale is highly dependent on the temperature profile and assumed methane humidity structure, which is not well established by the prior analysis, and (5) the rejection of the compact cloud layer models stated in the KT09 paper, was not on the basis of characteristics of optimized models that closely fit the observed spectra, but rather on the basis of general characteristics. While the KT09 model provides a good fit to the observations, it is far from clear how well that model is constrained, and to what degree other models could also fit the observations.

Issues regarding the vertical and latitudinal distribution of methane on Uranus. There are two features that have important effects on the observed spectrum of Uranus. One is the "above cloud" mixing ratio profile, and the other is the "deep" mixing ratio. There is a considerable range available from the set of solutions Lindal et al. (1987, JGR 92, 14987-15001) derived to match the observed refractivity profile at the latitude of the occultation (2-7^o S). These range from A (no methane) to F (4% deep methane), and only D, E, and F have any methane at all above the nominal cloud top. The cloud inferred from refractivity was centered at 1.2 bars and had a scale height of 2-4 km. Previously, we attempted to determine the methane mixing ratio by finding which of the Lindal solutions allowed cloud models to provide the best match to the observed spectrum. This made sense at low latitudes near those in which the occultation was measured, but was not appropriate at other latitudes because variations in methane mixing ratio would be accompanied by temperature structure variations that would imply large vertical wind shears, as well as violating observed constraints on latitudinal variations in temperature. KT09 assumed that the T(P) profile was invariant with latitude, but allowed the methane mixing ratio of the deep atmosphere to vary, which creates density variations with latitude that also lead to vertical wind shears (Sun et al., Icarus 91, 154-160, 1991). If these density gradients extend to great depths, the resulting implied wind fields would be in conflict with observations; thus the latitudinal gradients in methane, if present, cannot extend to great depths.

From the stratosphere to the cloud level, KT09 assumed a methane profile that did not vary with latitude, primarily based on the relatively flat latitudinal profile seen in the strongest methane bands, and adopted a methane mixing ratio profile that had humidity decreasing with altitude, using the functional form $RH=48\%[1-(1-P)^2]$, where P is the pressure in bars, but used only for $P<1.15$ bars. They claimed that a constant humidity profile would require more aerosol opacity between 0 and 0.5 bar than between 0.5 and 1 bar, which they deemed to be unphysical based on the haze modeling work of Rages et al. (1991, Icarus 89, 359-376). However, this does not seem to be a compelling argument because some component of the haze could evaporate at the warmer temperatures present at the higher pressures. In fact there solution, even for the decreasing humidity case, does have a total opacity above the 0.1 bar level comparable to that between 0.1 and 0.9 bar; which is also a violation of the Rages et al. model. Perhaps a better argument for a decreasing humidity profile is that the low stratospheric mixing ratio is compatible with a very low humidity at the tropopause level (about 12%).

Another factor that increased the methane mixing ratio for a given assumed humidity is that KT09 did not use any of the Lindal et al. temperature profile solutions, but chose one even warmer than the warmest F profile. To match their mixing ratio profile, using the model F T-P profile, we used a function of the form $RH = RH_{max} (RH_{min}/RH_{max})^{\wedge} [(1-P_{max}/P)/(1-P_{max}/P_{min})]$ separately applied over two regions: for 0.1 bar < P < 1 bar, we used RH_{min}=12% and RH_{max}=65%; and for 1 bar < P < 1.13 bars, we used RH_{min}=65% and RH_{max}=76%. This yields a methane mixing ratio at the troposphere of 1E-5, which is in agreement with the stratospheric value of Orton et al. (1987, Icarus 70, 1-12), but leads to notably greater methane mixing ratios near 1 bar than even Lindal's model F solution. To arrive at a methane profile that was enhanced as much as the K-T profile, but still satisfied radio occultation requirements, required us to reconsider the assumptions and analysis techniques on which the Lindal et al. solutions were based.

Combined reanalysis of Voyager radio occultation results and STIS spectra. Using most of the vertical cloud structure inferred by KT09, but replacing their diffuse middle tropospheric haze layer with two compact layers, we show (on the next page) that the upper compact layer could match both the STIS spectra and the Voyager refractivity profile using a He volume mixing ratio (VMR) of 0.116 and a methane VMR near 4%. The alternative cloud structures of KT09 and Sromovsky et al. 2011 (Icarus 215, 292-312) are compared in the following figure for 5° S. The putative methane cloud sheet near 1.2 bars has an optical thickness of about 0.3, and a particle radius near 1.2 μm, assuming conservative Mie scattering for this layer. The middle tropospheric cloud sheet near 1.7 bars has an optical depth of about 1.3, assuming the same scattering properties as assumed by KT09 for their diffuse layer. This is the most prominent layer inferred from near-IR observations of Irwin, et al. (2010, Icarus 208, 913–926), as indicated by the dashed line in the below figure. These two compact layers are well constrained by the spectral observations, but the compact deep layer we used is not well constrained, allowing optical depth and pressure to trade off over a wide range. The difference

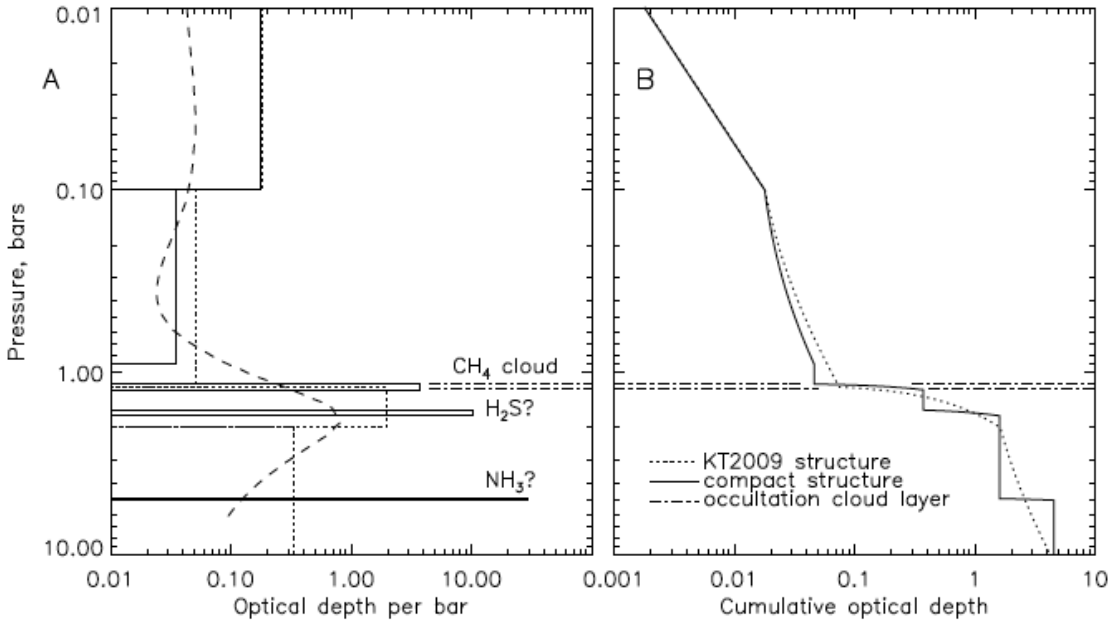

between the compact and diffuse cloud models becomes less apparent when their cumulative vertical optical depths are compared, as in panel B. The spectral observations alone cannot distinguish these options, but the compact version is a better match to the occultation results.

In our reanalysis of the occultation results, we first recreated the refractivity profile from the published temperature and methane structure for the Lindal et al. model D, then inverted the refractivity to different temperature and methane profiles using different assumptions about the methane constraints and considering different He/H_2 mixing ratios within the approximate range of its uncertainty. By reducing the mixing ratio of He slightly we were able to increase the mixing ratio of methane enough to yield methane saturation in the region of the putative cloud layer, and to have a higher methane mixing ratio above the cloud layer that was in better agreement with the rather high mixing ratio profile assumed by KT09. We created a suite of solutions with different He mixing ratios and used STIS spectra to constrain the results. To characterize methane absorption at CCD wavelengths we used the coefficients of KT09. We considered two models of vertical aerosol structure, as illustrated in the figure on page 5. The diffuse model has the KT09 structure, which provides a fitting standard of comparison. The compact model, the main feature of which is the splitting of the middle tropospheric layer of KT09 into two layers, allows us to see if a compact layer of methane particles can provide good fits to the observed spectra, and which occultation-derived profiles of temperature and methane mixing ratio provide (1) the best fit to the spectra and (2) the best agreement between the fit pressure for the middle tropospheric layer and the pressure inferred from the occultation analysis. Hopefully, the best spectral fit would occur for the same profile that provided the best pressure match. As shown in the above right figure, that is roughly what happened. The best overall spectral fit covers wide range of 2.9-4.9% CH4, while the best fit in the spectral region near 0.825 μm, where H_2 collision induced opacity is important favors 3.8-4.9% CH_4. The best match between putative methane cloud pressures inferred from spectra and

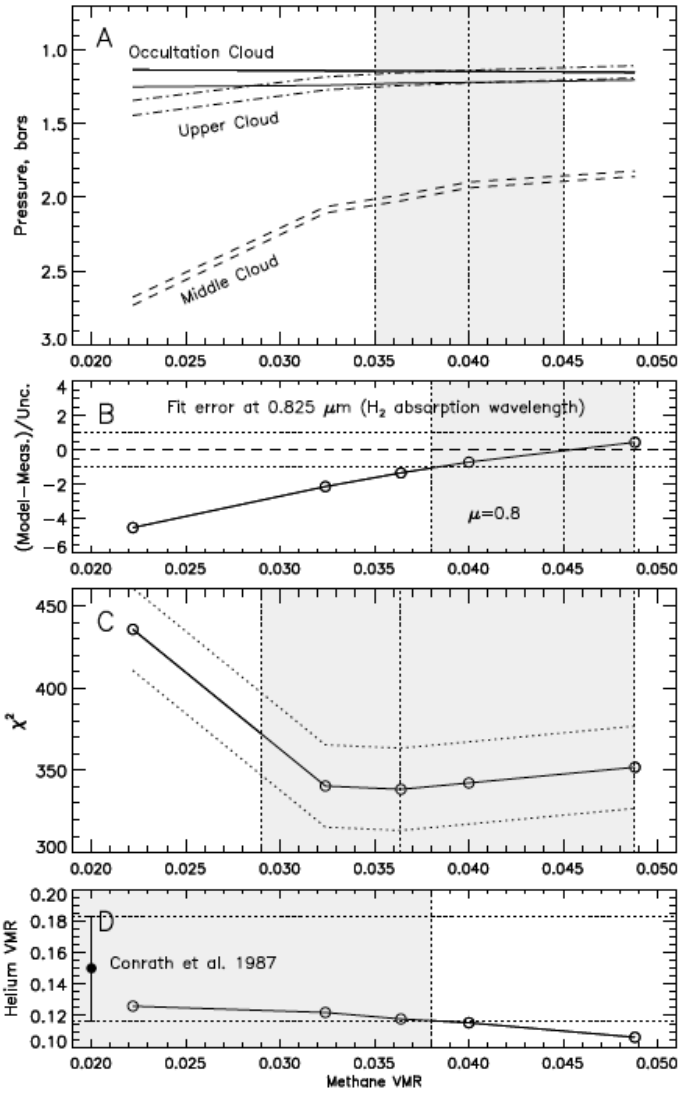

from occultation analysis is for 3.5-4.5% CH_4. In the figure, panel A displays the upper two compact layers inferred from fitting STIS spectra as a function of CH_4 mixing ratio (dashed and dot-dash) compared to the methane cloud boundaries inferred from occultation analysis; panel B displays the fit error at 0.825 μm, where CIA is dominant; panel C displays the overall spectral fit quality for the 0.6-1 μm spectral range; and panel D displays the He volume mixing ratio compared to the Conrath et al. (1987, JGR 92, 15003-15010) value and its uncertainty. The figure is from Sromovsky, et al., (2011, *Icarus* **215**, 292-312).

Latitudinal variations in methane profiles on Uranus.
The spectral observations we used to investigate latitude dependence are the calibrated spectral data cubes of KT09, which were derived from Hubble Space Telescope observations made in 2002 at nearly zero phase angle. The center-to-limb scans at each wavelength at each latitude of interest were fit to a smoothly varying empirical function, which we then interpolated to the same set of zenith angle cosines (0.3, 0.4, 0.6, and 0.8), providing both spectral and angular constraints on the cloud band at each latitude. This yielded a reduced noise, as did our spectral averaging over a boxcar of 36 cm−1. Our attempts to fit STIS observations with the same methane vertical distribution and the same vertical temperature structure derived for the occultation latitude were very successful over a wide range of latitudes (20° N to 30° S), with little variation in the compact cloud model parameters except for a declining optical depth towards the northern hemisphere and little variation in the quality of the fits. The fit quality was measured by the overall c^2 value for the entire spectral range from 0.55 to 1.0 μm, by the c^2 value at 0.825 μm, which is where the collision-induced absorption of H_2 is prominent, and by the linear fit error at 0.825 μm at a zenith angle cosine of 0.8 (for deepest penetration). But at higher southern latitudes overall fit quality and especially the fit quality near 0.825 μm both deteriorated dramatically as latitudes increased towards the south pole. To achieve a reasonable fit quality we needed to reduce the methane mixing ratio in the upper troposphere by a significant factor, confirming previous results of [2]. We tried to constrain the degree of depletion and depth of depletion using a variety of methane profiles. Those shown in the below left figure provided the best overall fits, though slightly different profiles, similar those of Karkoschka and Tomasko, (2011, Icarus 211, 780-797), can also provide reasonable fits. This depletion suggests a meridional circulation illustrated by the below right figure, in which methane-moist gas

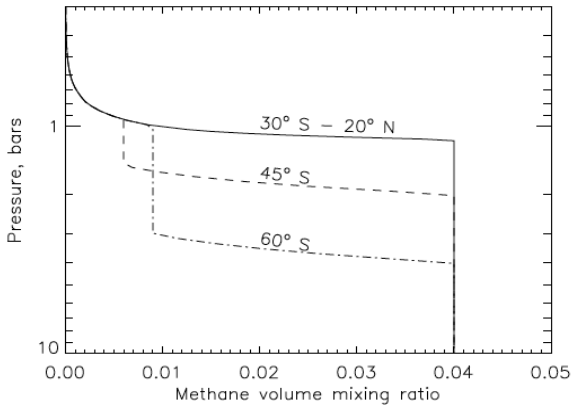

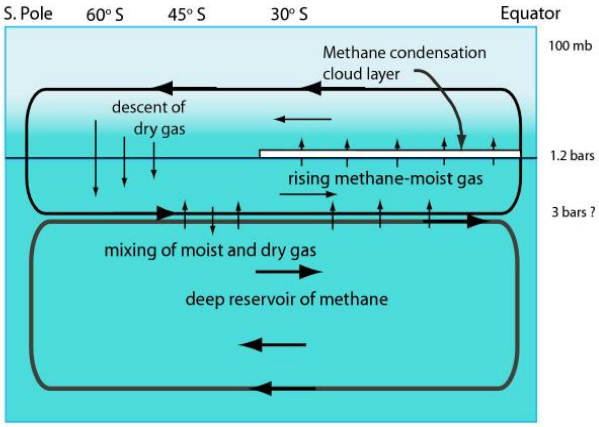

rising at low latitudes is dried out by the cold trap, where it forms a thin methane ice cloud. In this conceptual model the return flow involves descent of this dry gas at high latitudes, causing a local reduction in the methane mixing ratio to the depth of the descent.

Near-IR modeling of methane absorption. This research was carried out to provide a firmer foundation for analysis of near-IR observations of the ice giants. Before 2006 it was not possible to model near-IR spectra of Uranus and Neptune because of poor estimates of low temperature absorption of methane for weak bands that were important on these planets because of their large methane mixing ratios and relatively low aerosol content. A big improvement in near-IR modeling of Uranus was obtained using the band model of Irwin et al. 2006 (Icarus, 181, 309–319). However, that band model is based on laboratory measurements that must be significantly extrapolated to reach outer planet conditions of temperature, pressure, and path length. Observations by the Descent Imager/Spectral Radiometer (DISR) during the Huygens Probe descent to the surface of Titan provided a new constraint on band models, though it was of lower resolution than the 10 cm−1 of the band models, and was limited to wavelengths less than 1.6 μm. Using this constraint as well as other constraints, including lab and HST observations, an improved band model was constructed by Karkoschka and Tomasko (2010, Icarus 205, 674–694), providing significantly increased window absorption lacking in the Irwin et al. band model. But even these improvements were suspect for use in the deep atmospheres of Uranus and Neptune.

Ideally, line-by-line (LBL) calculations should be capable of defining the true dependence of absorption on temperature, pressure, and path length, provided sufficient numbers of lines are characterized to allow computation of all but a tiny fraction of the total absorption. The key parameters are the frequency, groundstate energy, and pressure-broadened line widths. In addition, because, at high pressures, window regions can be affected by the tails of nearby strong lines, it becomes necessary to know the line shape function in the far wing region, sometimes several hundred cm−1 from the center of the line. Furthermore, the temperature dependence of the pressure broadened line width is also needed. Unfortunately not all of this information is available for every line in the line databases. In many cases, line widths are assumed to be constant, and far-wing line shapes need to be constrained by observations. Thus, it is not immediately obvious whether our current improved line databases will actually be better than band models, even in regions where there are sufficiently many lines. Where LBL calculations can be verified they provide the tremendous advantage of high spectral resolution that cannot be matched by band models. Recent improvements in the measurement of methane absorption lines at wavenumbers in the region between 4800 cm^{-1} and 7700 cm^{-1} have greatly increased the number of lines with known ground-state energies, the number of weak lines, and the number of lines observed at low temperatures. This has made it possible to create a low-temperature line list that allows modeling near IR spectra of Titan using line-by-line calculations instead of band models (e.g. Bailey et al. 2011, Icarus 213, 218-232). To address deficiencies of the Bailey et al. compilation, we made a number of additions and modifications. The most important were to (1) replace lines in the 6165-6750 cm^{-1} range with line data from Wang, et al. (2011, J. Quant. Spec. & Rad. Trans.112, 937–951, (2) add lines from Mondelaine et al. (2011, Phys. Chem. Chem.

Phys. 13, 7985–7996) in the 1.28 μm transparency region, and (3) incorporate both room-temperature and 80 K lines to allow a wider range of utility. Compared to HITRAN 2008

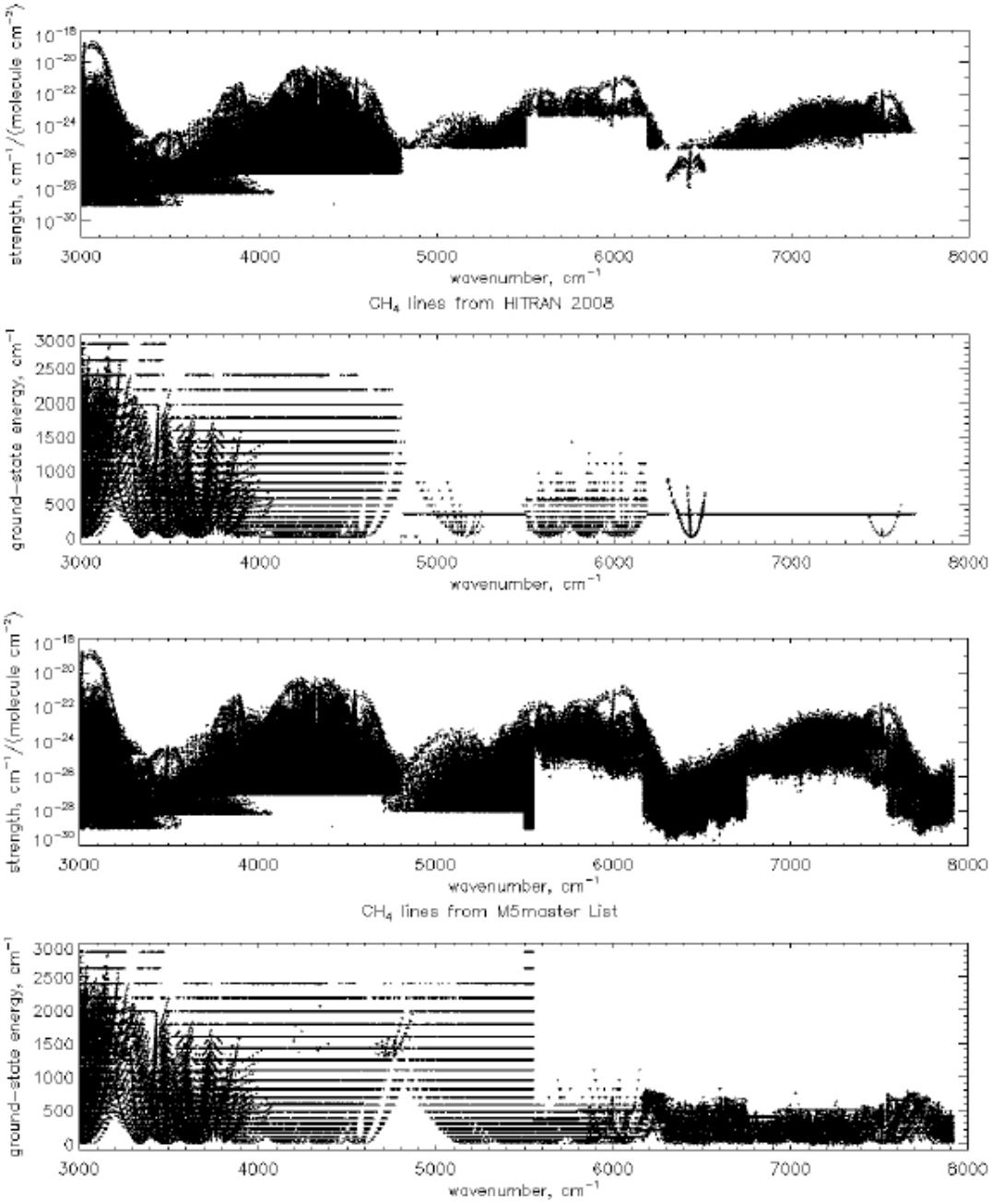

our line list provides much better coverage of low strength lines and has much better information on ground-state energies for the lines at shorter wavelengths, as shown in the above figure. The following figure compares the two band models with line-by-line calculations using our augmented line list (red) and the HITRAN 2008 line list (blue). For these conditions the two band models are in close agreement, and the augmented line list provides vast improvements over HITRAN between 5000 cm−1 and 7900 cm−1. The disagreements between LBL and band models in the 5000-5500 cm−1 region is likely due to the absence CH3D line data in this region, while the band models do account for

CH3D absorption. For Uranus conditions temperatures are lower and path lengths are much longer, resulting in disagreements between band models in the more transparent regions, but generally good agreement between KT09 and our LBL calculations. All models agree well in the strong bands. Under Saturn conditions ammonia fills in the transparent regions, and the presence of methane in greater abundance in the stratosphere (no cold trap) produces some disagreement in the strong bands, where significant opacity is here reached at fairly low pressures. Similar comments apply to Jovian conditions.

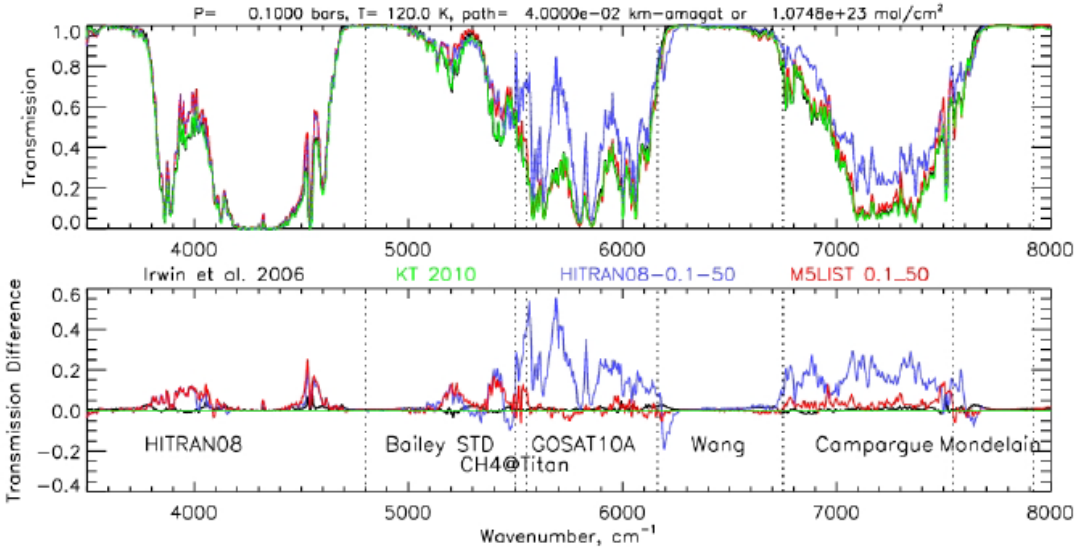

Deriving cloud pressures from near-IR H and Hcont observations. Although STIS spectra provided good constraints on cloud bands, with the help of center-to-limb as well as spectral information. The contrast of discrete features is very low at visible wavelengths, and obtaining center-to-limb information is much harder when trying to acquire spectral information at the same time. Using the inherently higher contrast at near-IR wavelengths, which allows detection of more features at higher S/N ratios, and often higher spatial resolution than is possible from HST, we made an effort to determine the pressure of discrete cloud features from the ratio of the I/F signals they created in two different filter bands that were centered at nearly the same wavelength, but had very different penetration depths due to their different sampling of methane absorption. The difference between background and cloud signals for the

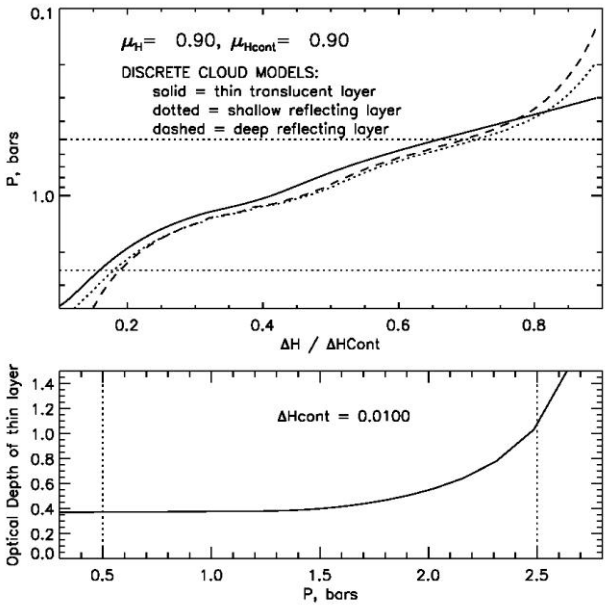

H filter divided by the same difference for the Hcont filter can be used as a barometer for locating the pressure of the cloud perturbation that produces the I/F change recognized as a discrete feature. This is illustrated in the top panel of the above figure. The bottom panel shows how the magnitude of the I/F change produced by a cloud can be used to estimate the corresponding optical depth change once the pressure is found. A sample set of H and Hcont (and K') images of the southern Berg feature obtained in 1996 is provided below. We used those images to estimate cloud pressures along the center of the Berg and at locations indicated by labeled outlines.

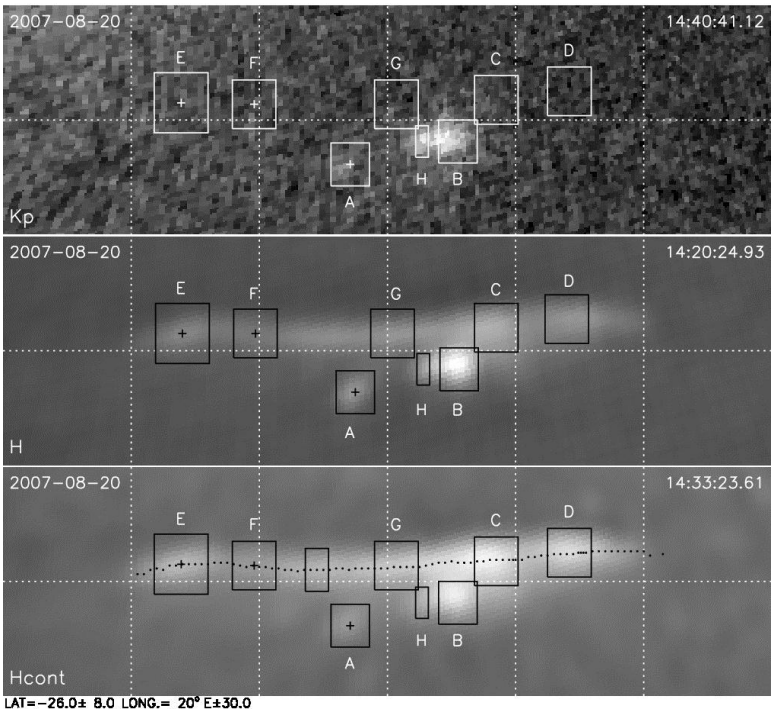

The cloud pressures and optical depth changes inferred from the H/ Hcont differential ratios are plotted in the below figure. We see that a few clouds extend above the methane condensation level (at 1.2 bars), and those are also visible in the K' image. But most

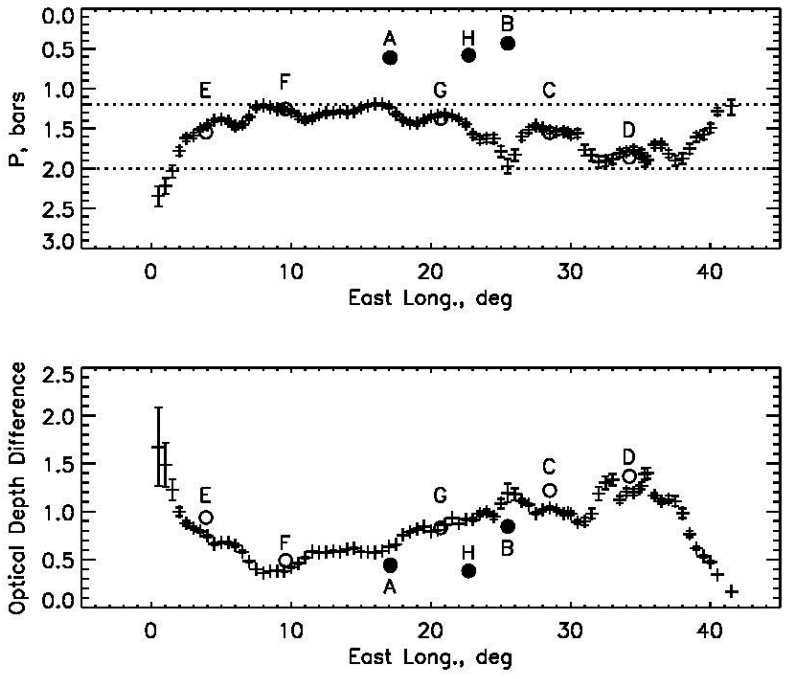

aerosols for this feature appear to reside between 1.2 bars and 2 bars, which is the main cloud layer identified by KT209. A plausible constituent for these clouds is H2S. These cloud altitude results are from the Kim et al. paper in preparation, which will require support from an external grant to bring to completion. The technique was also applied in the in-press Icarus paper by Sromovsky et al. (2012).